Pergamon

Int. J. Solids Structures Vol. 31, No. 5, pp. 599–611, 1994

0020–7683/94 $6.00 + .00

ON INTERACTING BRIDGED-CRACK SYSTEMS

K. X. HU, A. CHANDRA and Y. HUANG
Department of Aerospace and Mechanical Engineering, The University of Arizona, Tucson, AZ 85721, U.S.A.

(*Received* 16 *April* 1993; *in revised form* 16 *August* 1993)

Abstract—The analysis of a material containing multiple interacting bridged cracks is the principal objective of this paper. The traction-consistency equations in terms of bridging tractions and pseudo-tractions are developed to enable the decomposition of a problem involving multiple bridged cracks into a number of sub-problems, each involving only a single crack. Bridging law equations are formulated so that the bridging tractions and pseudo-tractions appear as primary unknowns. The current approach is capable of handling multiple interacting crack systems with a general form of bridging laws, linear or nonlinear, isotropic or anisotropic. Both isotropic and anisotropic bridging laws are investigated. It has been observed that the bridging law for a crack can significantly modify the tip behavior of the crack itself, while its influence on neighboring cracks is relatively weak. The influence of bridging anisotropy on crack-tip stress fields is found to be significantly modulated by the loading condition. Bridging effects and interaction effects on stress amplification and retardation are also examined. For nonlinear bridging, a case of fiber pull-out in metal/ceramic laminates is studied to establish the critical ratio of fiber-to-matrix thickness that would avoid single-crack extensions and transfer the deformation, instead, to multiple cracking. For multiple cracking situations, the crack nucleation sites are also predicted.

1. INTRODUCTION

In recent years, intermetallics and ceramic matrix composites have been used ever increasingly for high-temperature applications. However, the presence of microdefects can cause significant strength and modulus degradations of these materials. The growth and coalescence of microdefects manifest themselves as macrodefects and cause eventual failure of the component. In order to increase the fracture toughness of these relatively brittle compounds, methods studied by a number of researchers rely on bridge toughening, transformation toughening, fiber reinforcements, and microcrack toughening. For example, the fiber pull-out in unidirectional fiber-reinforced composites or fiber cross-over in randomly fiber-reinforced composites can provide bridging tractions to a level sufficient to retard a crack growth. For intermetallic aluminides, especially those of titanium, which have been identified as potential candidates for near-term success in high-temperature applications, the fracture toughness depends to a large extent on bridging mechanisms in the form of ductile phase accommodation and blunting, shear ligament toughening, and twin toughening. A bridge toughening mechanism for ductile particles dispersed in a brittle matrix was discussed by Sigl *et al.* (1988). The bridging was observed to be associated with particles intercepted by the crack. Such particles, well bonded to the matrix, exhibit significant plastic stretching in a zone of crack bridging, until they fail by a ductile mechanism. Important for the effectiveness of bridge toughening is the fact that a growing crack is attracted to the phase with the lower elastic modulus. As observed by Bao and Suo (1992), the bridging mechanism provides a unified treatment for the cohesive forces that hold material together, ranging from atomic bonding to fiber cross-over.

Many publications have been devoted to the modeling of bridged cracks. These may be broadly classified as traction and dislocation formulations. In the traction formulation, the crack opening displacements are obtained in terms of bridging tractions, which in turn can be solved with a proper bridging law (Marshall *et al.*, 1985; Marshall and Cox, 1987; Rose, 1987; Budiansky *et al.*, 1988; McCartney, 1987; Bao and Hui, 1990; and Cox and Lo, 1992). The distribution-of-dislocation approach takes advantage of the widely used crack modeling technique and solves the system in terms of crack opening gradients (Bao and Suo, 1992; Hu *et al.*, 1993a). For bridged cracks, the traction approach is appealing, since a bridging law usually implies a relationship between bridging tractions and crack

opening displacements. However, this approach has been applied, so far, only to the analysis of a single bridged crack. As was observed by a number of researchers (Shaw *et al.*, 1993 and Beyerde *et al.*, 1992), multiple cracking occurs in composite materials, such as metal/ceramic laminates, and can be used as a mechanism for damage redistribution, consequently enhancing the toughness of the brittle ceramics. Moreover, various bridging mechanisms and their interactions with renucleated and distributed cracks will significantly influence further damage development and determine the final macrofailure mode of the structure. Accordingly, the analysis of a material containing multiple interacting bridged cracks is the principal objective of this paper. In Section 2, a formulation capable of modeling general multiple interacting bridged-crack systems is developed based on bridging tractions and pseudo-tractions. Anisotropic bridging, inherent to multiple crack systems, is also discussed in detail. Although superposition is used to form the basis of the analysis, the analysis can incorporate the nonlinearity of the bridging law since the nonlinearity is treated through the bridging law only. Section 3 focuses on the effects of bridging anisotropy and crack interactions on the propagation of interacting cracks in the case of linear bridging. Section 4 examines a case of nonlinear bridging, i.e. the fiber pull-out in a metal/ceramic composite. The critical ratio of fiber-to-matrix thickness is established that would avoid single-crack extensions and transfer the deformation, instead, to multiple matrix cracking. The crack nucleation sites are also predicted for the case of multiple matrix cracking. A summary of results and a brief discussion of systems involving large-scale bridging and real-life components with microstructures are presented in Section 5.

2. MODELING OF INTERACTING BRIDGED-CRACK SYSTEMS

2.1. *Problem statement*

This section presents an approach to the analysis of a system containing multiple interacting bridged cracks. As shown schematically in Fig. 1, it is assumed that M bridged

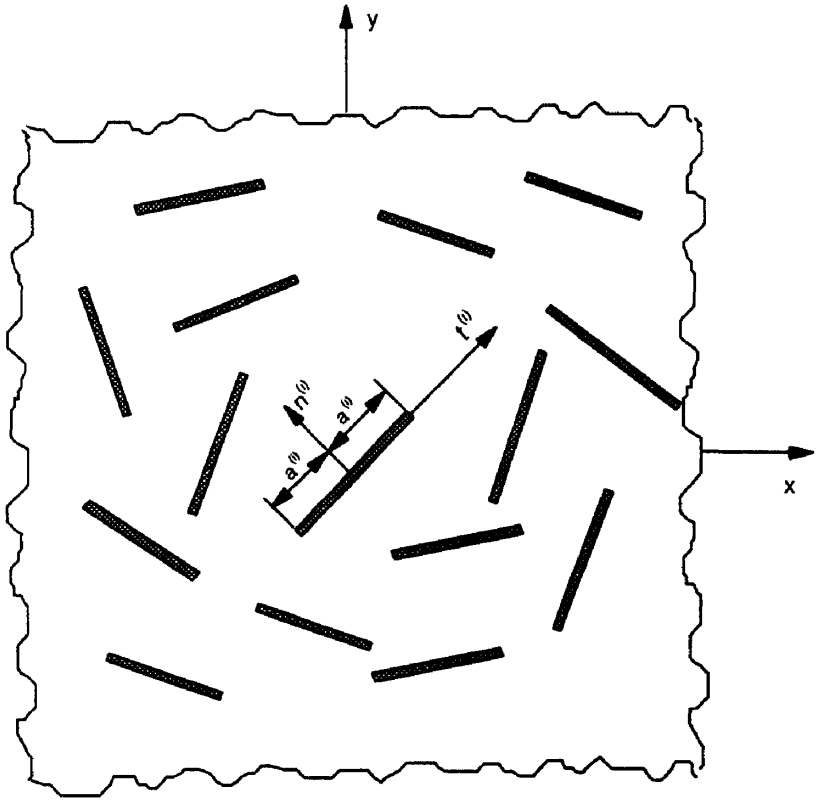

Fig. 1. Schematic diagram of an interacting bridged-crack system.

cracks of arbitrary orientations are embedded in a matrix material with shear modulus G and Poisson's ratio v. With respect to global Cartesian coordinates x and y, we consider a local tangential-normal coordinate system with the origin at the center of the ith crack. The normal direction and the tangential direction along the ith crack are denoted by $n^{(i)}$ and $t^{(i)}$. The occupancy of the ith crack is denoted as $-a^{(i)} < t < a^{(i)}$. Under certain applied loading conditions, crack bridging occurs and (however sophisticated the mechanisms involved) can be represented as a distribution of closing tractions on each individual crack surface. Bridging tractions can be related to the corresponding crack opening displacements through a bridging law,

$$p_t = f_t(u_t, u_n), \tag{1a}$$

$$p_n = f_n(u_t, u_n), \tag{1b}$$

where p_t and p_n are bridging tractions and u_t and u_n are crack opening displacements in the tangential and normal directions, respectively. It should be noted that a specific form of the bridging law can be obtained in light of the micromechanical mechanisms for a particular bridging situation (Marshall *et al.*, 1985; McCartney, 1987; Hutchinson and Jensen, 1990; Needleman, 1987, 1990; and Tvergaard, 1990, 1992, for more details). As pointed out by Bao and Suo (1992), it is the variation of a scalable quantity associated with the bridging law, not the bridging law itself, that accounts for the richness in material behavior, ranging from the scale of a few nanometers for atomic bonding to about a meter for cross-over fibers.

Various bridging laws can be broadly classified into categories such as linear and nonlinear bridging and isotropic and anisotropic bridging, among others. Isotropic bridging is, by definition, independent of crack orientations and can be found in particulate-reinforced composites, fiber-reinforced composites with random fiber cross-over, and intermetallics with second-phase agents. Anisotropic bridging becomes an important issue in the analysis of systems involving multiple interacting cracks since the orientation dependence of a bridging law is naturally brought to light due to the variation in crack orientations. Anisotropic bridging can occur, for example, in a unidirectional fiber-reinforced composite with pull-out fibers. Furthermore, the bridging law can assume different forms in each individual crack, i.e. bridging can be crack-wise inhomogeneous.

2.2. *Integral equations*

Following a superposition technique proposed by Horii and Nemat-Nasser (1985), the system is divided into as many sub-problems as there are cracks, each sub-problem containing a single crack in the infinitely extended matrix. A distribution of unknown tractions, s_t and s_n, is placed on the corresponding crack surface in each sub-problem. The unknown tractions, also called pseudo-tractions, will be determined in such a way that all the requirements of the original interacting bridged-crack problem are satisfied. Based on this superposition observation, fundamental solutions for an infinite body containing a single crack, subject to a pair of concentrated tangential loads and a pair of concentrated normal loads of opposite direction on the crack surface, are required for the current analysis. The fundamental solutions for these cases were obtained by Tada *et al.* (1985) in terms of Westgaard complex potentials. The stress and displacement fields can be easily constructed thereafter.

Let us now consider the effects of all cracks on the mth crack. For consistency, stress fields associated with different cracks should be transformed to the local tangential-normal coordinate system for the mth crack, $(t^{(m)}, n^{(m)})$. Contributions of all M cracks to the stress field at the presumed location of the mth crack are now represented by their corresponding unknown distribution of pseudo-tractions. Summing the effects of all cracks on the mth crack and imposing the traction conditions that are consistent with the original interacting bridged-crack problem, we get:

$$s_n^{(m)}(t^{(m)}) - \sum_{\substack{i=1 \\ i\neq m}}^{M} \int_{-a^{(i)}}^{a^{(i)}} [K_{11}(t^{(m)}, t^{(i)}) s_t^{(i)}(t^{(i)}) + K_{12}(t^{(m)}, t^{(i)}) s_n^{(i)}(t^{(i)})] \, dt^{(i)} + \sigma_{nn}^{(m0)}(t^{(m)}) - p_n^{(m)}(t^{(m)}) = 0 \quad m = 1, \ldots, M, \quad (2a)$$

and

$$s_t^{(m)}(t^{(m)}) - \sum_{\substack{i=1 \\ i\neq m}}^{M} \int_{-a^{(i)}}^{a^{(i)}} [K_{21}(t^{(m)}, t^{(i)}) s_t^{(i)}(t^{(i)}) + K_{22}(t^{(m)}, t^{(i)}) s_n^{(i)}(t^{(i)})] \, dt^{(i)} + \sigma_{tn}^{m0}(t^{(m)}) - p_t^{(m)}(t^{(m)}) = 0 \quad m = 1, \ldots, M, \quad (2b)$$

where $\sigma_{nn}^{(m0)}$ and σ_{tn}^{m0} are the stress components at the location of the mth crack under the applied loading condition, but in the absence of all cracks, and $p_t^{(i)}$ and $p_n^{(i)}$ are the distributions of unknown bridging tractions and $s_t^{(i)}$ and $s_n^{(i)}$ are the distributions of unknown pseudo-tractions in the tangential and normal directions, respectively, corresponding to the ith crack. Kernels K_{11} through K_{22} are deduced, from the fundamental solution, and details on the construction of these kernels, following a similar approach, can be found in Hu *et al.* (1993b). Although these kernels are lengthy, they carry distinct physical meaning. For example, $K_{12}(t^{(m)}, t^{(i)})$ represents the normal stress σ_{nn} (in the local coordinate system of the mth crack) at a particular point $t^{(m)}$ on the presumed mth crack location due to the normal component (in the local coordinate system of the ith crack) of the force at a particular point $t^{(i)}$ on the ith crack. Other kernels may be interpreted similarly.

The bridging law equations are considered next. To this end, the crack opening displacements in eqn (1) must be obtained for the original interacting bridged-crack problem. We note, however, that the crack opening displacements of the mth crack can only be induced by the pseudo-tractions, $s_t^{(m)}$ and $s_n^{(m)}$, on the mth crack (the tractions on all other cracks do not contribute to any separations along the presumed location of mth crack). The crack opening displacments on the mth crack can then be easily obtained in terms of the unknown pseudo-tractions $s_t^{(m)}$ and $s_n^{(m)}$:

$$u_n^{(m)}(t^{(m)}) = \int_{-a^{(m)}}^{a^{(m)}} K_{33}(t^{(m)}, t^{(i)}) s_n^{(m)}(t^{(i)}) \, dt^{(i)} \quad m = 1, \ldots, M, \quad (3a)$$

$$u_t^{(m)}(t^{(m)}) = \int_{-a^{(m)}}^{a^{(m)}} K_{44}(t^{(m)}, t^{(i)}) s_t^{(m)}(t^{(i)}) \, dt^{(i)} \quad m = 1, \ldots, M, \quad (3b)$$

where the kernels K_{33} and K_{44} also bear a distinct physical meaning. For example, K_{33} represents the crack opening at a particular point $t^{(m)}$ on the mth crack by the application of a unit point normal load at a point $t^{(i)}$ on the mth crack. Details on the kernels K_{33} and K_{44} are given explicitly by Tada *et al.* (1985).

Equations (1)–(3) now provide an integral equation representation of interactions in a general system containing M bridged cracks. It is noted that the equilibrium equations of the stress state at any internal point are exactly satisfied through the nature of the built-in fundamental solutions. The traction-consistency conditions, as represented in eqns (2a, b), and the bridging law equations, as represented in equations (1a, b) and (3a, b) will have to be satisfied approximately through a numerical solution of integral equations.

When the boundary conditions for cracks are assumed traction-free, the bridging effects vanish and the bridged-crack system degenerates to a system of interacting traction-free cracks. The traction-consistency equations alone provide the solution to such problems (see Hori and Nemat-Nasser, 1987 and Hu *et al.*, 1993b, for more elaborations on the traction-consistency equations). On the other hand, when the interacting bridged cracks become isolated or only a single crack exists, the effects of interactions disappear and the system reduces to the case of a single bridged crack.

2.3. *Numerical solution scheme*

It can be observed that the traction-consistency eqns (2a, b) are well-behaved and that singularity occurs only in the kernels K_{33} and K_{44} for crack opening equations (3a, b). Moreover, the singularity in K_{33} and K_{44} is a weak one and only in a logarithmic form, which can easily be handled by numerical integration. We adapt a Gauss quadrature approach. After normalizing the integration interval to $(-1, 1)$ and collocating the quadrature points, the discretized traction-consistency equations become:

$$s_n^{(m)}(t_j^{(m)}) - \sum_{\substack{i=1 \\ i\neq m}}^{M} a^{(i)} \sum_{k=1}^{N} [K_{11}(t_j^{(m)}, t_k^{(i)}) s_t^{(i)}(t_k^{(i)}) + K_{12}(t_j^{(m)}, t_k^{(i)}) s_n^{(i)}(t_k^{(i)})] w_k$$

$$+ \sigma_{nn}^{(m0)}(t_j^{(m)}) - p_n(t_j^{(m)}) = 0 \quad i = 1, \ldots, M; j = 1, \ldots, N, \quad (4a)$$

$$s_t^{(m)}(t_j^{(m)}) - \sum_{\substack{i=1 \\ i\neq m}}^{M} a^{(i)} \sum_{k=1}^{N} [K_{21}(t_j^{(m)}, t_k^{(i)}) s_t^{(i)}(t_k^{(i)}) + K_{22}(t_j^{(m)}, t_k^{(i)}) s_n^{(i)}(t_k^{(i)})] w_k$$

$$+ \sigma_{tn}^{(m0)}(t_j^{(m)}) - p_t(t_j^{(m)}) = 0 \quad i = 1, \ldots, M; j = 1, \ldots, N. \quad (4b)$$

The crack opening equations can be regularized in the following fashion:

$$u_n^{(m)}(t_j^{(m)}) = a^{(m)} \sum_{\substack{k=1 \\ k\neq j}}^{N} K_{33}(t_j^{(m)}, t_k)[s_n^{(m)}(t_k) - s_n^{(m)}(t_j^{(m)})] w_k$$

$$+ \frac{2(1-\nu)}{G} \sqrt{a^{(m)2} - t_j^{(m)2}}\, s_n^{(m)}(t_j^{(m)}) \quad j = 1, \ldots, N, \quad (5a)$$

$$u_t^{(m)}(t_j^{(m)}) = a^{(m)} \sum_{\substack{k=1 \\ k\neq j}}^{N} K_{44}(t_j^{(m)}, t_k)[s_t^{(m)}(t_k) - s_t^{(m)}(t_j^{(m)})] w_k$$

$$+ \frac{2(1-\nu)}{G} \sqrt{a^{(m)2} - t_j^{(m)2}}\, s_t^{(m)}(t_j^{(m)}) \quad j = 1, \ldots, N, \quad (5b)$$

where N is the number of quadrature points, $t_j^{(m)}$ and $t_k^{(i)}$ are collocation and integration points, and w_k is the Gauss weight in the normalized interval $(-1, 1)$. As was observed by Delves and Mohamed (1985), the Gauss quadrature is the most efficient and accurate approach to the numerical solution of integration equations if logarithmic singularity is not present. The regularization of logarithmic kernels used here ensures a level of accuracy similar to that for regular kernels.

Several important features of the integral equation formulation may be noted here. First, after substituting the crack opening equations into the bridging law, the governing equations can be expressed in terms of unknown bridging tractions and pseudo-tractions only. Second, when the cracks degenerate into conventional traction-free ones, the traction-consistency equations alone give the solution. Unlike the commonly used distribution-of-dislocation approach or other types of force or displacement formulations, the present approach does not present any singularity, thus ensuring a high level of accuracy in numerical solutions. Third, the problem is reduced to a number of single-crack problems. This will facilitate the evaluation of physical quantities, such as crack-tip stress intensity factors. Moreover, the level of sparseness in the final coefficient matrix is enhanced, allowing efficient solution of the system. Finally, the dimension of the final coefficient matrix is primarily dictated by the traction-consistency equations. It is observed that the influence of one crack on another is a strong function of the distance between them. Accordingly, by deciding on zones of influence for individual cracks (depending upon desired accuracies), a banded structure with reduced size may be obtained for the final coefficient matrix.

3. LINEAR BRIDGING

The effects of linear bridging on the stress field of interacting cracks are investigated in this section. The proposed integral equation approach can handle arbitrary orientations and distributions of a large number of cracks. Following a treatment by Kachanov (1985), the current approach may be formally applied to intersecting cracks. Particular focus is placed on several aspects, such as crack interactions, crack bridging and bridging anisotropy.

Two collinear cracks of equal length, a, are considered first. It is assumed that the surface of the crack is traction-free (or nonbridging) and is subject to a remote tension, σ_0, perpendicular to the crack-line. The stress intensity factors (SIFs) of the near tip are listed in Table 1 for different numbers of integration points. It is seen that the current approach can yield very accurate results using fewer quadrature points than the commonly employed distribution-of-dislocation approach. For example, 10 integration points can provide the normalized SIFs with an error of less than 1% for a crack-tip separation of $t/2a = 0.0125$.

The interactions among bridged cracks are considered next. As mentioned before, anisotropic bridging deserves particular attention for interacting cracks with mutual orientations. In this context, we consider two specific types of bridging laws. First, we consider a special type of isotropic linear bridging and assume that the bridging can only sustain loading normal to the crack direction. The bridging law can then be expressed as:

$$p_n = \lambda_n u_n \quad \text{and} \quad p_t = 0 \tag{6a, b}$$

where λ_n is the proportionality constant. Second, we consider the case of an anisotropic linear bridging law and assume that the bridging can only sustain the loading in the y-direction of the fixed x–y coordinate system. The bridging law for a crack inclined to the x-axis with an angle α can be readily derived as:

$$p_n = \lambda_n \cos\alpha(u_n \cos\alpha + u_t \sin\alpha), \tag{7a}$$

$$p_t = \lambda_n \sin\alpha(u_n \cos\alpha + u_t \sin\alpha). \tag{7b}$$

It is noted that the bridging law depends explicitly on the crack orientation and is thus anisotropic.

The inset of Fig. 2(a) shows two cracks with a mutual orientation of an angle α, subject to a biaxial remote loading, $\sigma_{xx} = \sigma_{yy} = \sigma_0$. The distance between crack centers is fixed at $d/a = 2.1$. The variations of mode-I stress intensity factors (SIFs) of the inner tips for both left (fixed orientation in the x-direction) and right (inclined) cracks with the angle α are shown in Fig. 2(a) for the case of nonbridged cracks ($\lambda_n = 0$). The same configuration of bridged cracks with isotropic bridging (eqns 6a, b) and anisotropic bridging (eqns 7a, b) are also considered. The bridging strength is characterized by a dimensionless bridging constant, $c = 2(1-\nu)\lambda a/G$. Figures 2(b) and 2(c) show the variation of mode-I SIFs with the angle α for $c = 1.6$ and $c = 3.2$, respectively. Figure 2(a) (nonbridged cracks) provides a benchmark for an evaluation of the effectiveness of crack bridging. Comparisons of Figs 2(b) and 2(c) with Fig. 2(a) reveal that bridging can reduce the SIFs significantly. A large value of c is desirable to increase retardation of crack-tip stresses. This is certainly the case for long cracks (large values of a) and bridging agents with large values of λ. It is observed

Table 1. Inner-tip SIFs for two collinear cracks of equal length (t = tip separation/crack length)

		Current/dislocation		
t	Exact	$N = 10$	$N = 15$	$N = 25$
0.0125	2.782	2.755/2.512	2.775/2.705	2.782/2.776
0.0250	2.215	2.207/2.138	2.213/2.201	2.215/2.214
0.0500	1.795	1.793/1.780	1.795/1.794	1.795/1.795
0.1000	1.491	1.491/1.490	1.491/1.491	1.491/1.491
0.2500	1.229	1.229/1.229	1.229/1.229	1.229/1.229

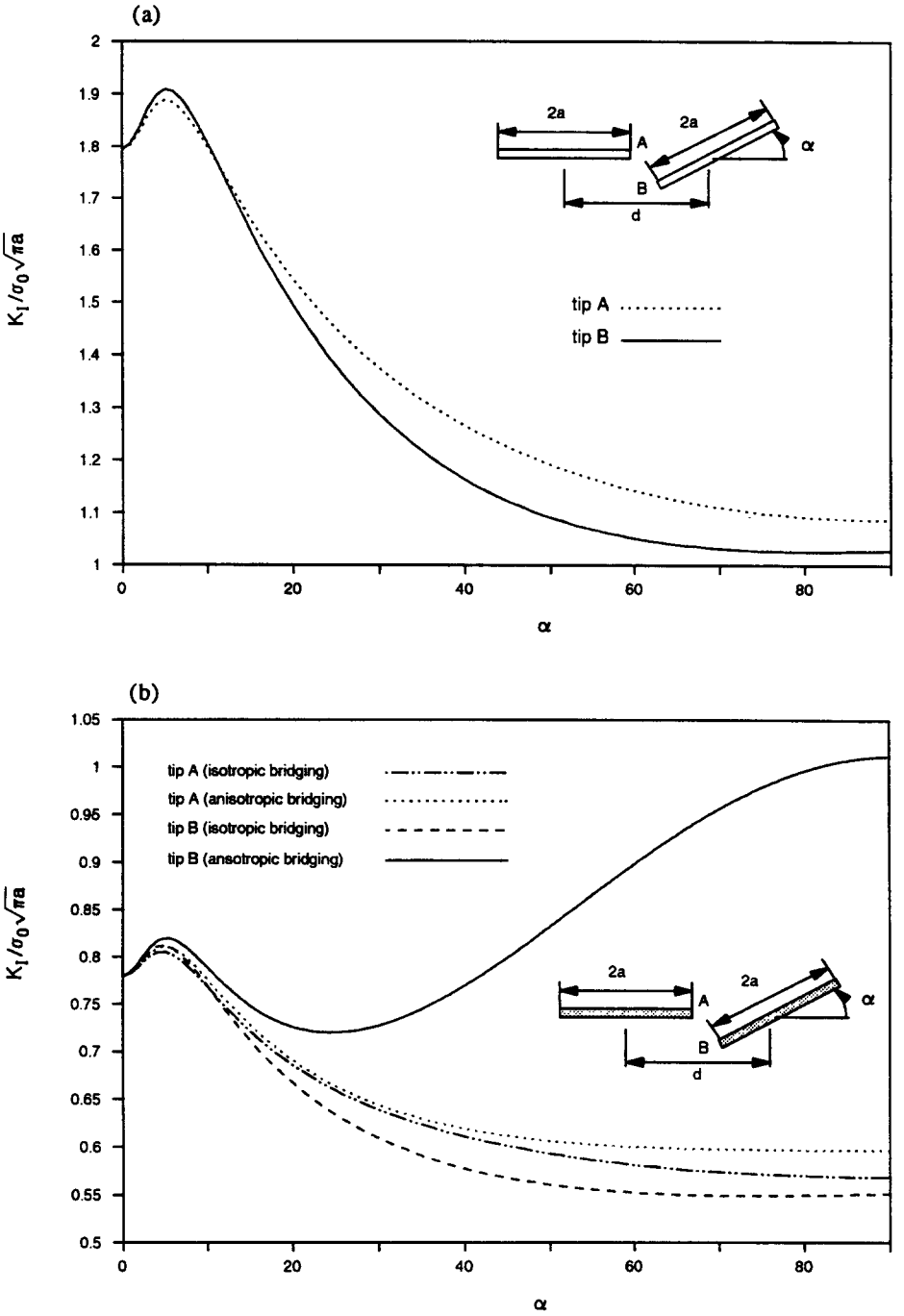

Fig. 2. Variation of mode-I SIFs with orientation for biaxial remote loading, $\sigma_{xx} = \sigma_{yy} = \sigma_0$, and $d/a = 2.1$: (a) $c = 0$: (b) $c = 1.6$; (c) $c = 3.2$.

from Figs 2(b) and 2(c) that the SIFs at tip A do not indicate much difference between isotropic bridging and anisotropic bridging, suggesting that crack-tip behavior can be altered only to a limited extent by changing the bridging law of a neighboring crack. The difference in SIFs between isotropic and anisotropic bridging, however, is pronounced for crack tip B. For example, the normalized SIFs at $\alpha = 45°$ and $c = 1.6$ and 0.57 and 0.80 for isotropic and anisotropic bridging, respectively. It is also noted that anisotropy complicates the variation of SIF for crack tip B. The tip-B SIF reaches a local maximum first at a small value of angle α, then it drops to a minimum value before it goes up again.

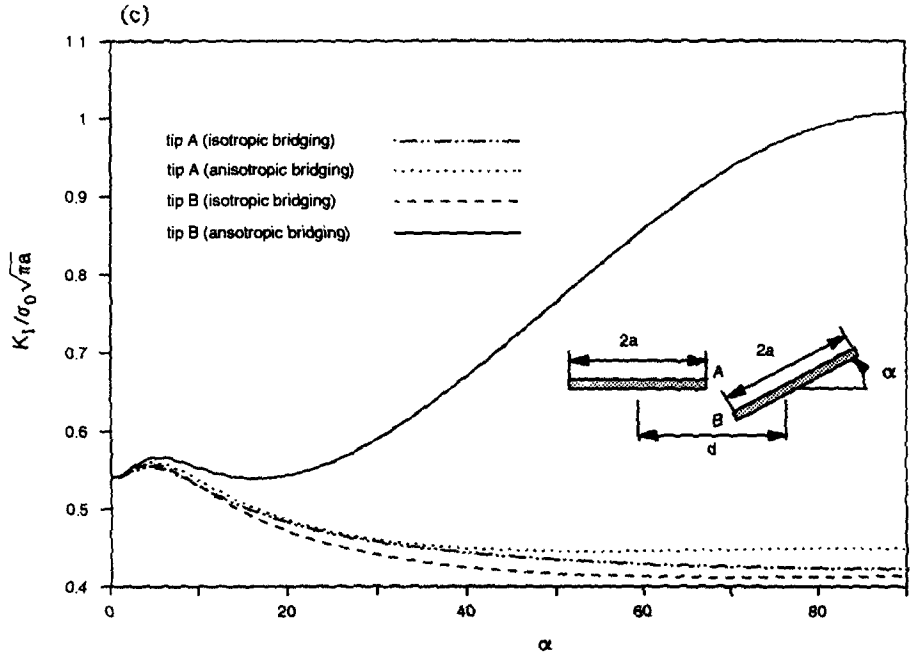

Fig. 2.—*Continued.*

Obviously, the existence of the local maximum SIF at small α is *due to crack interactions*, and the existence of the minimum value is largely due to the effect of anisotropy.

The effects of anisotropy, as shown in Figs 2(b) and 2(c) are significant for crack tip *B* for the case of biaxial remote loading ($\sigma_{xx} = \sigma_{yy} = \sigma_0$). However, this is not the case for uniaxial remote loading ($\sigma_{yy} = \sigma_0$). Figure 3 considers the same configuration as in Fig. 2(b) ($c = 1.6$), but a uniaxial remote loading ($\sigma_{yy} = \sigma_0$) is applied. It is seen that isotropic and anisotropic bridging produce almost identical SIFs for both crack tips *A* and *B*. We

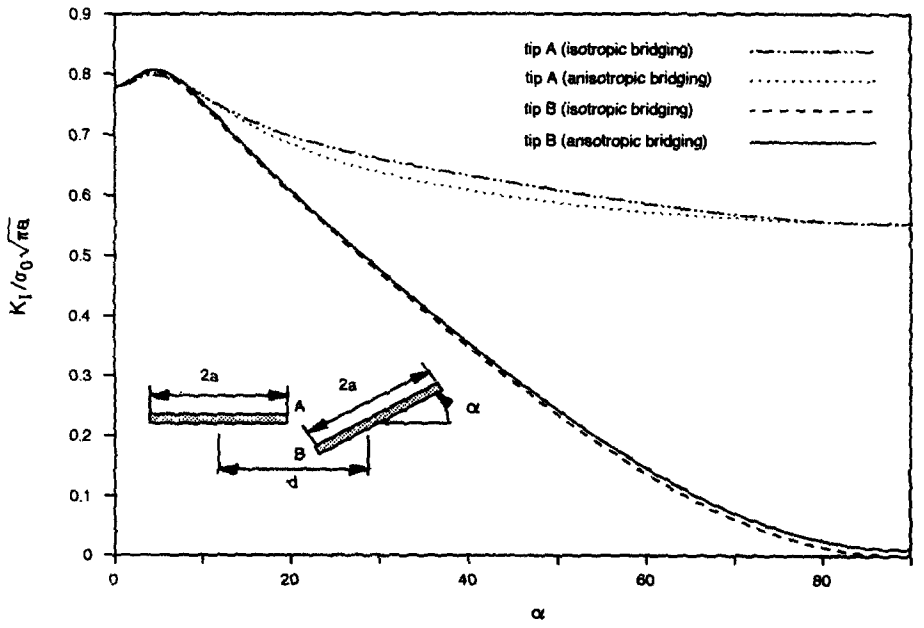

Fig. 3. Variation of mode-I SIFs with orientation for uniaxial remote loading, $\sigma_{yy} = \sigma_0$, $d/a = 2.1$, and $c = 1.6$.

can conclude that the effect of bridging anisotropy on crack-tip stress can be large or small, depending on the loading conditions.

Figures 4(a) and 4(b) consider three parallel, offsetting cracks, one being stepped up from the other. The system is subject to a remote tension, σ_0, in the direction perpendicular to the crack. As observed by Beyerde *et al.* (1992), the stepped cracks occur in unidirectional fiber-reinforced composites due to a damage redistribution process of multiple cracking. In such cases, the effect of bridging forces must be considered. As a first approximation to the analysis of multiple cracking of a unidirectional fiber-reinforced composite, we employ the

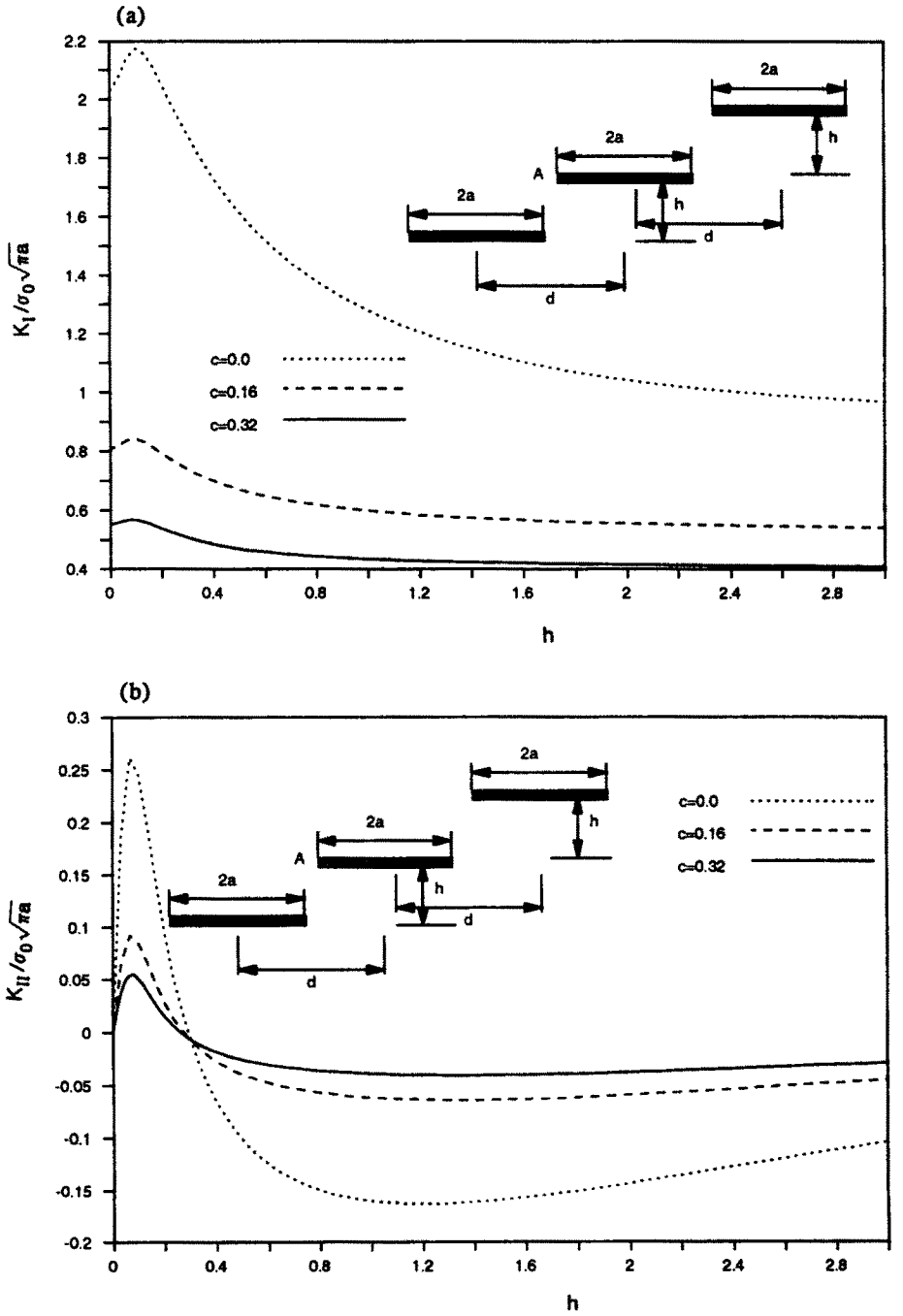

Fig. 4. Variation of the inner-tip SIFs of the central crack with step for three parallel, offsetting, interacting bridged cracks; a remote tension, σ_0, in the direction perpendicular to the cracks is applied to the system and $d/a = 2.1$: (a) mode-I; (b) mode-II.

bridging law in eqn (6). Due to interactions between the cracks, the mode-I [Fig. 4(a)] and mode-II [Fig. 4(b)] SIFs of the central crack vary in a complex fashion with the step height. It is also noted that there is a considerable level of mode-II deformation, which is solely induced by the interactions in this case. Bridging consistently retards the strength of the crack-tip stress field for both mode-I and mode-II deformations.

4. NONLINEAR BRIDGING FOR FIBER PULL-OUTS

Shaw and Evans (1993) studied the nucleation of a microcrack in ceramics across a metal layer in metal/ceraminc laminates. Ceramics are brittle and vulnerable to microcracking, while the plastic flow in metals dissipates the stress concentration in metal layers to avoid microstructural damage and to provide the toughness for a composite. As shown in Fig. 5, a pre-existing crack in a metal/ceramic laminate may result in stress concentration ahead of the crack tip, thereby nucleating a microcrack along the crack plane in the next ceramic layer. As observed by Dalgleish *et al.* (1989) and Cao and Evans (1991), the renucleated crack may penetrate the ceramic layer and be arrested by two neighboring metal layers. In such laminates, the metal layers, particularly the ones near the dominant crack tip, provide the bridging forces to retard crack extension. As an approximation to this problem, we consider a discrete bridging model over a single metal layer right behind the crack tip [see Fig. 5(a)]. Following the approach of Marshall *et al.* (1985) and its modification by Hutchinson and Jensen (1990), a bridging law can be stated as:

$$p_n = \lambda\sqrt{u_n}, \quad p_t = 0 \qquad \text{over } a - t_m - t_f < t < a - t_m, \tag{8}$$

where λ is a material constant depending on the sizes, the moduli, and the interfacial frictional properties of the metal and ceramics layers. It should be noted that the bridging law given in eqn (8) was derived for fibers frictionally bonded to the matrix. As noted by the work cited above, it can be equally applied to a metal/ceramic layer system. When broken layers dominate the process, however, softening will have to be accounted for and the bridging law should be modified accordingly.

After crack renucleation, two modes of damage evolution are possible: (i) multiple cracking in the same ceramic layer, or (ii) extension of the dominant crack through the metal interface into the next ceramic layer. Shaw *et al.* (1993) observed that, subsequent to crack renucleation, relatively thick ceramic layers lead to damage in the form of continuous microcracking in the adjacent ceramic layers (i.e. single-crack extension) while thin ceramic layers cause the formation of multiple parallel stacked cracks with a zone near the dominant crack (i.e. multiple cracking). The formation of a multiple-cracking zone distributes damage and significantly enhances the composite toughness as compared to the extension of a dominant crack (Deve and Maloney, 1991; Deve *et al.*, 1992; Hu and Chandra, 1993).

The problem here is to determine quantitatively the critical thickness of ceramic layers (or the ratio of ceramic-to-metal thickness), below which multiple cracking prevails over single-crack extension in metal/ceramic laminates. For the configuration shown in Fig. 5(a), the maximum stress in the ceramic layer occurs somewhere (point B) above the crack plane, say, the step height h_c. This maximum stress, $\sigma_{\max}$, is compared to the stress, σ_0, at point A on the crack plane in the next unbroken layer. If $\sigma_{\max}$ is larger than σ_0 and reaches the level of the ceramic breakage stress, σ_c, the next microcrack will be renucleated at the site of $\sigma_{\max}$, i.e., somewhere above the dominant crack in the same ceramic layer. Therefore, multiple cracking dictates the process. If $\sigma_{\max}$ is less than σ_0, the next microcrack will be nucleated in the next unbroken ceramic layer along the crack plane such that single-crack extension is prevalent. Based on this reasoning and the bridging law given in eqn (8), the critical ratio of ceramic-to-metal thickness can be obtained, and we can also predict the site where the next microcrack will nucleate for the case of multiple cracking. Figure 5(b) shows the critical ratio with a dimensionless constant $\bar{\lambda} = [t_m\lambda^2(1-\nu)]/G\sigma_c$. Figure 5(c) gives the prediction of the site of the next microcrack nucleation in the case of multiple cracking. It is noted that the critical ratio and the nucleation position can be characterized through only

a single configuration constant if a/t_m is fixed. In the current analysis, the calculation of σ_{max} is made along the centerline of the ceramic layer. Other types of approximations might be performed; for example, one may average the stress over the ceramic layer at different attitudes to obtain σ_{max}.

5. DISCUSSION AND CONCLUSIONS

The problem of interacting bridged cracks was considered in this paper. The analysis is based on a superposition technique that allows the decomposition of a multiple bridged-crack system into a number of sub-problems, each involving only a single crack. The

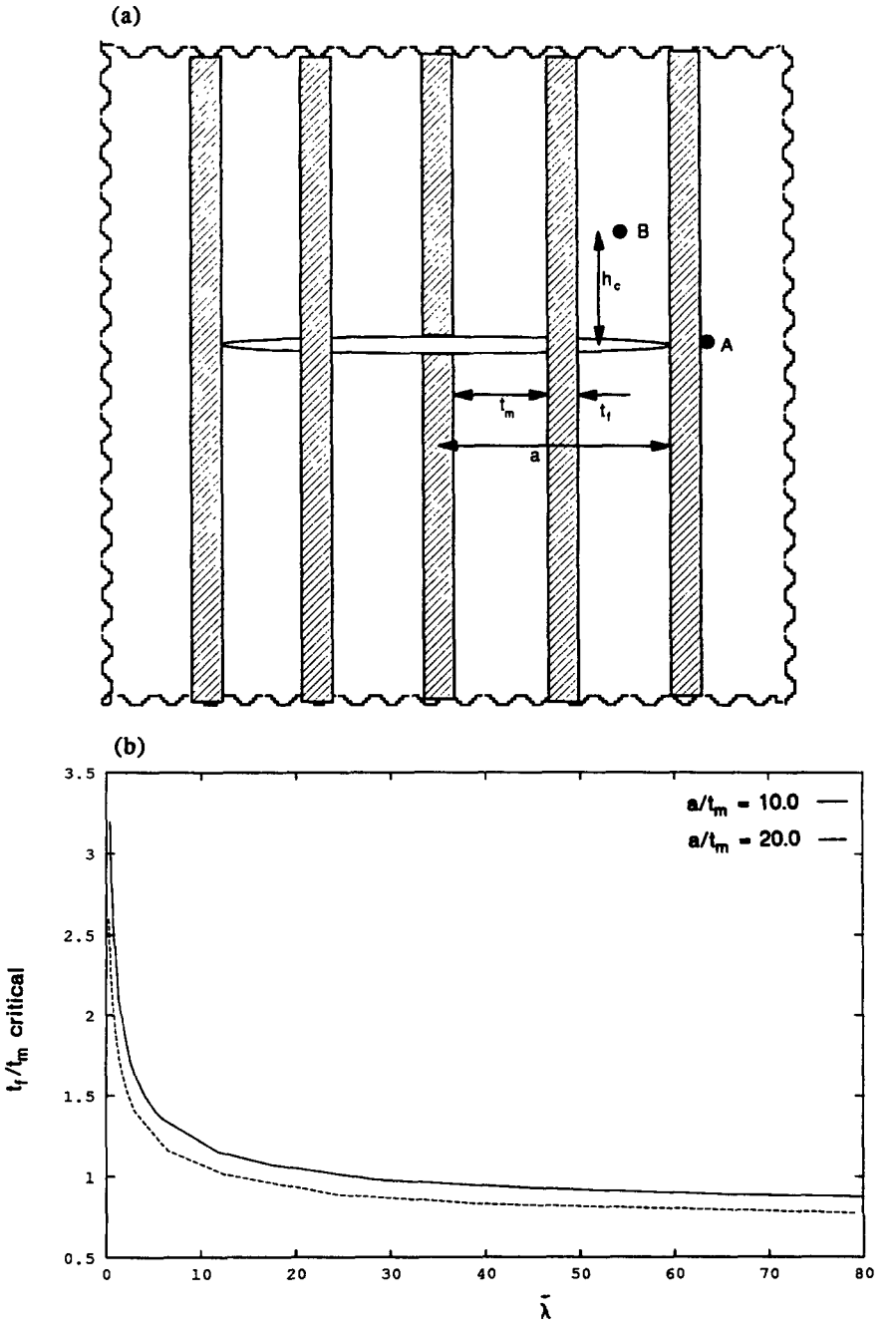

Fig. 5. A metal/laminate with a bridged crack: (a) schematic diagram; (b) variation of the critical ratio of the ceramic-to-metal layer thickness with the dimensionless configuration constant $\bar{\lambda}$; (c) variation of the predicted step height, h_c, at which a microcrack will be nucleated, with the dimensionless configuration constant $\bar{\lambda}$.

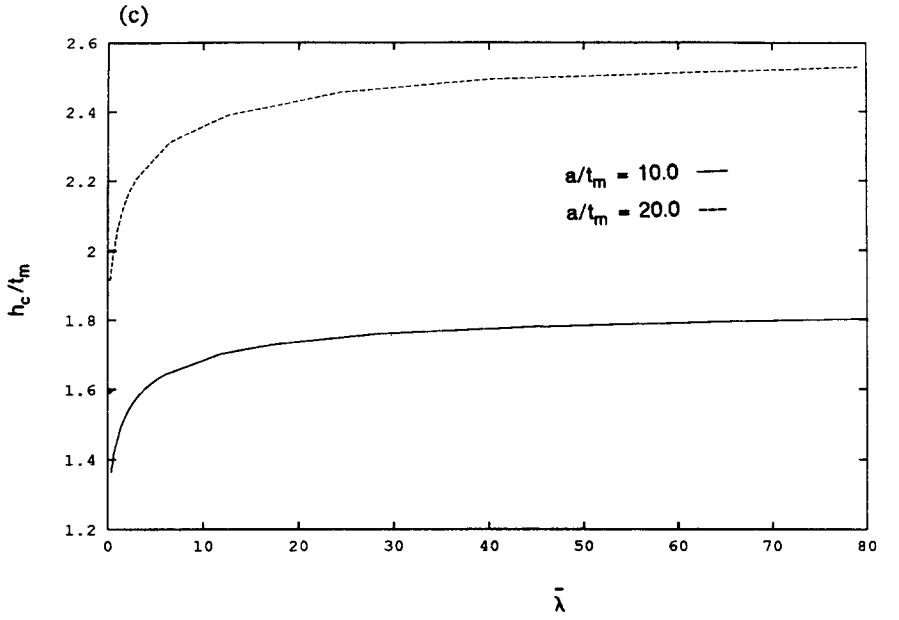

Fig. 5.—*Continued.*

superposition spawns the traction-consistency equations in terms of bridging tractions and pseudo-tractions, which are solved as primary unknowns. The secondary unknowns, such as stress and strain fields, can be constructed through direct integration. The current approach is capable of handling multiple interacting crack systems with a general form of the bridging law, linear or nonlinear, isotropic or anisotropic. Anisotropy in the bridging law, which becomes an important issue for multiple bridged-crack systems, is investigated to show that the change in a crack bridging law from isotropic to anisotropic can modify the tip behavior of the crack itself to an extent, depending on the loading conditions. Nevertheless, a crack-tip stress field can be altered, only to a limited extent, by changing a bridging law in a neighboring crack. Bridging effects and interaction effects on stress amplification and retardation were also examined and revealed several interesting aspects. For nonlinear bridging, a case of fiber pull-out in metal/ceramic laminates was studied to establish the critical ratio of fiber-to-matrix thickness that leads to the arrestation of a single-crack extension and transfers it to multiple cracking. The prediction was also made for the position of the crack nucleation site in the case of multiple cracking. These predictions were characterized through a single configuration parameter.

In composite materials, the defects always coexist with reinforcements. Modeling of interactions of cracks with various forms of bridging can provide bounding estimates, such as maximum available retardation, for microstructure design. In applications to real-life structures, one must incorporate general loading situations, finite and often complex geometries of particular components, as well as a detailed representation of interacting microstructures and the associated damage evolution. And therein lies the fundamental difficulty in the analysis of these problems. Typically, the microstructures and their spacings are of the order of a few micrometers, while the overall dimensions of a component may range from a few centimeters to even a meter. Thus, a computational scheme is required, simultaneously, to provide a detailed representation of the underlying mechanics at two widely different scales: a local micro-scale with interacting microstructures, and a global macro-scale representing the real structure's configuration. The current analysis is capable of yielding a fundamental solution that accounts for the microstructural interactions. This fundamental solution can be augmented through the boundary integral equation approach

to provide a solution to the problem of real-life structures. Also, the framework of large-scale bridging was recently discussed by Bao and Suo (1992). Work on large-scale bridging and the development of computational methods with emphasis on the connections among microstructural interactions, finite geometries, and realistic boundary conditions for real-life structures will constitute a part of our future endeavors.

Acknowledgements—The authors gratefully acknowledge the financial support provided by the U.S. National Science Foundation under Grant No. DMC 8657345.

REFERENCES

Bao, G. and Hui, Y.-C. (1990). Effects of interface debonding on the toughness of ductile-particle reinforced ceramics. *Int. J. Solids Structures* **26,** 631–642.

Bao, G. and Suo, Z. (1992). Remarks on crack-bridging concepts. *Appl. Mech. Rev.* **45,** 355–366.

Beyerde, S., Spearing, S. M. and Evans, A. G. (1992). Damage mechanisms and the mechanical properties of a laminated 0/90 ceramic composite. *J. Am. Ceram.* **75,** 3321–3330.

Budiansky, B., Amazigo, J. C. and Evans, A. G. (1988). Small-scale crack bridging and the fracture toughness of particulate-reinforced ceramics. *J. Mech. Phys. Solids* **36,** 167–187.

Cao, H. C. and Evans, A. G. (1991). On crack extension in ductile/brittle laminates. *Acta Metall.* **39,** 2997–3005.

Cox, B. N. and Lo, C. S. (1992). Load ratio, notch, and scale effects for bridged cracks in fibrous composites. *Acta Metall. Mater.* **40,** 69–80.

Dalgleish, B. J., Trumble, K. P. and Evans, A. G. (1989). The strength and fracture of alumina bonded with aluminum alloys. *Acta Metall.* **37,** 1923–1931.

Delves, L. M. and Mohamed, J. L. (1985). *Computational Methods for Integral Equations.* Cambridge University Press, Cambridge.

Deve, H. E., Evans, A. G. and Shih, D. (1992). A high-toughness gamma-titanium aluminide. *Acta Metall.* **40,** 1259–1265.

Deve, H. E. and Maloney, M. J. (1991). On the toughening of intermetallics with ductile fibers: the role of interfaces. *Acta Metall.* **39,** 2275–2284.

Hori, M. and Nemat-Nasser, S. (1987). Interacting micro-cracks near the tip in the process zone of a macro-crack. *J. Mech. Phys. Solids* **35,** 601–629.

Horii, H. and Nemat-Nasser, S. (1985). Elastic fields of interacting inhomogeneities. *Int. J. Solids Structures* **21,** 731–745.

Hu, K. X. and Chandra, A. (1993). A fracture mechanics approach to the strength degradation in ceramic grinding processes. *ASME J. Eng. Ind.* **115,** 73–84.

Hu, K. X., Chandra, A. and Huang, Y. (1993a). Crack-fiber-interface interactions. *Mech. Mater.* (submitted).

Hu, K. X., Chandra, A. and Huang, Y. (1993b). Multiple void-crack interaction. *Int. J. Solids Structures* **30,** 1473–1489.

Hutchinson, J. and Jensen, H. M. (1990). Models of fiber debonding and pullout in brittle composites with friction. *Mech. Mater.* **9,** 139–163.

Kachanov, M. (1985). A simple technique of stress analysis in elastic solids with many cracks. *Int. J. Fracture* **28,** R11–R19.

Marshall, D. B. and Cox, B. N. (1987). Tensile fracture of brittle matrix composites: influence of fiber strength. *Acta Metall.* **35,** 2607–2619.

Marshall, D. B., Cox, B. N. and Evans, A. G. (1985). Mechanics of matrix cracking in brittle matrix composites. *Acta Metall.* **33,** 2013–2021.

McCartney, L. N. (1987). Mechanics of matrix cracking in brittle fibre-reinforced composites. *Proc. Roy. Soc. Lond. A* **409,** 329–350.

Needleman, A. (1987). A continuum model for void nucleation by inclusion debonding. *ASME J. Appl. Mech.* **54,** 525–531.

Needleman, A. (1990). An analysis of tensile decohesion along an interface. *J. Mech. Phys. Solids* **38,** 289–324.

Rose, L. R. F. (1987). Crack reinforcement by distributed springs. *J. Mech. Phys. Solids* **35,** 383–405.

Shaw, M. C., Marshall, D., Dadkhah, M. S. and Evans, A. G. (1993). Cracking and damage in ceramic/metal multilayers. *Acta Metall.* **41,** 3311–3322.

Sigl, L. S., Matagga, P. A., Dalgleish, B. J., McMeeking, R. M. and Evans, A. G. (1988). On the toughness of brittle materials reinforced with a ductile phase. *Acta Metall.* **36,** 945–953.

Tada, H., Paris, P. C. and Irwin, G. R. (1985). *The Stress Analysis of Cracks Handbook.* Paris Productions, Inc., St. Louis, Missouri.

Tvergaard, V. (1990). Effect of fiber debonding in whisker-reinforced metal. *Mater. Sci. Eng. A* **A125,** 203–213.

Tvergaard, V. (1992). Effect of ductile particle debonding during crack bridging in ceramics. *Int. J. Mech. Sci.* **34,** 635–649.